The Host Galaxies of Radio-Loud AGN: The Black Hole–Galaxy Connection

Matthew O'Dowd[1]

Space Telescope Science Institute, 3700 San Martin Dr., Baltimore, MD 21218, USA; odowd@stsci.edu

C. Megan Urry

Department of Physics and Yale Center for Astronomy and Astrophysics, P.O. Box 208121, New Haven, CT 06520-8121, USA; meg.urry@yale.edu

Riccardo Scarpa

European Southern Observatory, Alonso de Cordova 3107, Vitacura, Casilla 19001, Santiago, Chile; rscarpa@eso.org

ABSTRACT

We have studied the host galaxies of a sample of radio-loud AGN spanning more than four decades in the energy output of the nucleus. The core sample includes 40 low-power sources (BL Lac objects) and 22 high-power sources (radio-loud quasars) spanning the redshift range $0.15 \lesssim z \lesssim 0.5$, all imaged with the high spatial resolution of HST. All of the sources are found to lie in luminous elliptical galaxies, which follow the Kormendy relation for normal ellipticals. A very shallow trend is detected between nuclear brightness (corrected for beaming) and host galaxy luminosity. Black hole masses are estimated for the entire sample, using both the bulge luminosity–black hole mass and the velocity dispersion–black hole mass relations for local galaxies. The latter involves a new method, using the host galaxy morphological parameters, μ_e and r_e, to infer the velocity dispersion, σ, via the fundamental plane correlation. Both methods indicate that the entire sample of radio-loud AGN are powered by very massive central black holes, with $M_\bullet \sim 10^8$ to $10^{10} M_\odot$. Eddington ratios range from $L/L_{Edd} \sim 2 \times 10^{-4}$ to ~ 1, with the high-power sources having higher Eddington ratios than the low-power sources. Overall, radio-loud AGN appear to span a very large range in accretion efficiency, which is all but independent of the mass of the host galaxy.

---

[1]also at School of Physics, University of Melbourne, Parkville, Victoria 3052, Australia

Subject headings: galaxies: active — BL Lacertae objects: general — quasars: general — galaxies: elliptical and lenticular, cD — black hole physics — galaxies: kinematics and dynamics

1. Introduction

Whether there is a link between the intrinsic power of Active Galactic Nuclei (AGN) and their host galaxies is not known. It seems plausible that more massive host galaxies might form in high density regions that also support the formation of more massive nuclear black holes (Small & Blandford 1992; Haehnelt & Rees 1993; Kauffmann & Haehnelt 2000) and/or that more massive host galaxies could support an increased rate of fuelling. For nearby, non-active galaxies there is observational evidence that the mass of the central supermassive black hole is correlated with bulge mass (Magorrian *et al.* 1998; van der Marel 1999a) and with bulge velocity dispersion (Ferrarese & Merritt 2000; Gebhardt *et al.* 2000). This could lead to an observable link between emission from the region around the black hole and the luminosity of the hosting galaxy, for example as observed by van der Marel (1999b) for local spheroids.

Several studies have indeed suggested nuclear luminosity might be related to host galaxy mass in AGN (McLeod, Rieke & Storrie-Lombardi 1999; Schade, Boyle & Letawsky 2000; Hooper, Impey & Foltz 1997); however, other studies find no such relation (Urry *et al.* 2000; McLure, Kukula & Dunlop 1999; Bahcall *et al.* 1997; Smith *et al.* 1986). Certainly among radio-loud AGN alone, for which the host galaxies are generally luminous ellipticals with well-defined morphologies, no trend has been detected in previous studies. This may be due to the fact that only a small range of (high) nuclear power has been probed in the past.

To make a clean comparison among AGN that differ only in nuclear output (rather than host galaxy morphology, dust content, star formation history, etc.), we restrict the present study to radio-loud AGN ($F_{5\ \mathrm{GHz}}/F_B > 10$; Kellerman *et al.* 1989). These are known to have relativistic jets formed near the central supermassive black hole (Urry & Padovani 1995), and so should be governed by similar physics near the black hole. Additionally, the early-type spectral energy distributions typical of the host galaxies (Ridgway & Stockton 1997; Scarpa *et al.* 2000a; McLure, Dunlop & Kukula 2000; Pentericci *et al.* 2001) make the K corrections straightforward.

Our goal is to probe the connection between AGN power (processes near the black hole) and environment (host galaxy properties) for radio-loud AGN over the full range of intrinsic nuclear power. Using BL Lac objects and Radio-Loud Quasars (RLQs) to represent

the extremes of this range, it is possible to define redshift-matched samples that span more than four orders of magnitude in intrinsic nuclear power. This range reflects a continuum of accretion powers, which in turn arise from some variation in the process of fuelling and/or jet formation near the black hole.

2. Matched AGN Samples and Data Corrections

The difficulty in comparing host galaxies over a wide range of nuclear power lies in the redshift selection bias. Most low-power AGN, namely FR I radio galaxies and Seyferts, are not found in complete samples beyond about $z \sim 0.2$. In contrast, samples with large numbers of quasars extend to $z \sim 0.5$ and beyond, and due to the steep luminosity functions of quasars, few appear at low redshift. Indeed, in any flux-limited AGN sample, there is an induced correlation between redshift and point-source luminosity. This can introduce apparent correlations between host galaxy and nuclear luminosities because galaxies evolve over even modest redshift ranges (Bressan, Chiosi & Fagotto 1994). If the redshift range is therefore restricted, the resulting sample will ordinarily span a narrow range in nuclear power, making it difficult to measure intrinsic trends that depend on nuclear power.

We avoid this fundamental difficulty by selecting a low-power sample for which intrinsic luminosity of the point source is not well correlated with observed (selection) luminosity, and for which samples exist to high redshift, namely, BL Lac objects. BL Lacs are intrinsically low-power blazars whose close alignment with the line of sight results in strong relativistic beaming of the jet emission, in many cases resulting in magnification of > 1000 times, and meaning that BL Lacs can be found in large numbers beyond $z \sim 1$, to the same redshift range at which luminous quasars can be found in large numbers. Their observed luminosity depends more on the Doppler factor than on intrinsic luminosity, thus the sample studied has no observed correlation of (intrinsic) nuclear brightness with host galaxy brightness.

We now describe the BL Lac subsample and the RLQ subsample selected for study.

2.1. The Low-Power Sample

We carried out an extensive HST imaging survey of 110 BL Lac objects with WFPC2, primarily in the F702W (R-band) filter.[2] These were a randomly selected subset of 132 BL

[2]Based on observations with the NASA/ESA Hubble Space Telescope, obtained at the Space Telescope Science Institute, which is operated by the Association of Universities for Research in Astronomy, Inc. under

Lacs from six complete samples (4 X-ray-, 1 radio-, 1 optically-selected) spanning the full range of observed BL Lac spectral properties. The complete HST-observed subsample of 110 BL Lacs covers a redshift range of $0.027 \leq z \leq 1.34$.

The host galaxy parameters were extracted by fitting a model galaxy profile plus a central point spread function (PSF) to the azimuthally-averaged image profile. Extensive testing on simulated data, and comparison to results from the two-dimensional analysis of a subsample has shown that this approach allows accurate measurement of the magnitude of both the host galaxy and nucleus and of the host galaxy scale radius, as well as allowing us to distinguish between a bulge- or disk-dominated galaxy profile. The excellent HST resolution proved to be vital in determination of the morphological parameters, as most of the critical information was within 0.5 – 1 arcseconds of the core. The full details of the image reduction and host galaxy fitting can be found in Scarpa *et al.* (2000) and the host galaxy results are presented in Urry *et al.* (2000).

Host galaxies were resolved in 65% of the sample, with 95% resolved for $z < 0.5$, and none resolved for $z > 0.7$. All resolved host galaxies with sufficient signal-to-noise ratios were well-fitted by a de Vaucouleurs profile (i.e., a bulge-dominated host), in preference to an exponential profile (i.e., a disk-dominated host). This strongly supports the idea that radio-loud AGN reside in elliptical galaxies rather than spirals. The average K-corrected absolute magnitude of the host galaxies from the entire HST-imaged sample is $M_R = -23.7 \pm 0.6$ mag (RMS dispersion).

To minimize the number of unresolved host galaxies (while still maintaining a useful redshift range), we restrict this sample to $z \lesssim 0.5$ for this comparison study. We further restrict the sample to $z \gtrsim 0.15$ to match the available quasar subsample (see below). The final low-power subsample consists of 40 objects with $0.15 \lesssim z \lesssim 0.5$.

2.2. The High-Power Sample

For the high-power comparison sample we take RLQs with published imaging data comparable in quality to the BL Lac sample. We exclude high-power radio galaxies (i.e., FR IIs) because their nuclear luminosities cannot be measured directly due to obscuration (Barthel 1989). Specifically, we limit the comparison sample to quasars that satisfy the following selection criteria:

NASA contract No. NAS5-26555.

- Published results from HST imaging data are available. Our extensive testing has shown that ground-based studies at intermediate redshifts can result in inconsistent measurements of host galaxy properties. The stability of the HST point spread function results in much more uniform data, and its superior resolution is critical for determining host morphological parameters.

- Restricted redshift range, $z \lesssim 0.5$. For this redshift range our detection rate of BL Lac host galaxies was 95%, so there is minimal bias against faint hosts with bright nuclei.

- Host galaxies detected for full sample studied. That is, $\sim 100\%$ of the RLQs with $z \lesssim 0.5$ in the published sample must have resolved host galaxies. As above, this avoids bias against low host-nuclear luminosity ratios.

We identified four quasar studies meeting these criteria: Dunlop et al. (2002), 10 objects; Boyce et al. (1998), 3 objects; Hooper et al. (1997), 6 objects; and Bahcall et al. (1997), 6 objects (see Table 1). The lowest RLQ redshift is $z = 0.15$, so we restrict the comparison sample to $0.15 \lesssim z \lesssim 0.5$. The final high-power sample consists of 22 RLQs (three RLQs have duplicate observations).

The BL Lac and RLQ subsamples have indistinguishable redshift distributions, with a Kolmogorov-Smirnov (K-S) test indicating a 37% probability of the same parent population. Thus the fundamental distinction between the two samples is nuclear luminosity.

2.3. Photometric and Cosmological Corrections

In order to compare the host galaxy properties measured in different studies, we first convert all results to the Cousin's R band, which is closest to the HST F702W filter. For consistency, we also used same cosmology as Scarpa *et al.* (2000): $H_0 = 50$ km/s/Mpc and $q_0 = 0$.

The spectral corrections were made using a spectral energy distribution (SED) derived from galaxy synthesis models (Bruzual & Charlot 1993, and private communication). Redshifted SEDs were convolved with the transmission curves for both the Cousin's R and the observed bands, and then normalised to the published host galaxy magnitudes. An early-type spectrum was assumed for all hosts, with a passively evolving population of age 8 Gyrs. Uncertainties in the spectral corrections are small because we are converting between similar filters. The uncertainties are highest in the case of the Bahcall *et al.* sample, of order a tenth of a magnitude, where we are correcting between the F606w filter (V band) and R band. Thus variations among the particular SEDs of different host galaxies should not affect

our results significantly. The corrected Cousin's R absolute magnitudes for the high-power subsample are given in Table 1. We used the average values for the two RLQs with duplicate observations.

3. Results

3.1. The Host Galaxies

The median K-corrected absolute magnitudes of the host galaxies of the subsamples differ slightly: $M_R = -23.75$ mag for the low-power subsample and $M_R = -24.2$ mag for the high-power subsample, with about half a magnitude of scatter about their means, which are -23.76 mag and -24.02 mag respectively. Figure 1 shows host galaxy absolute magnitude plotted as a function of redshift. The distributions of two subsamples overlap completely, though the low-power subsample tends to have slightly fainter (but still quite luminous) host galaxies. A K-S test indicates that the host galaxy magnitudes of these two subsamples are (marginally) unlikely to be drawn from the same parent luminosity distribution (4% probability).

In general, the host galaxies of the radio-loud AGN in this sample have similar luminosities to brightest cluster galaxies ($M_R = -23.9$ mag; Thuan & Puschell 1989). At their faintest they are ~ 0.5 mag above L^* (-22.4 mag; Efstathiou, Ellis & Peterson 1988). This places them within normal bounds for non-active elliptical galaxies, albeit at the bright end of the luminosity distribution. Every host galaxy in this sample for which the morphological parameters were measured (84% of the sample) was preferentially fit (and well fit) by a de Vaucouleur's profile, suggesting that they are in fact elliptical galaxies.

Normal (non-active) ellipticals exhibit a tight relationship between the log of effective radius (r_e) and surface brightness at that radius (μ_e), the so-called Kormendy relation ($\mu_e = A\ \log_{10} r_e + C$; Kormendy 1977), a projection of the Fundamental Plane. The slope and intercept of this relation depend on stellar dynamics (via the velocity dispersion, which is not known for this sample) and galaxy shape, size, and luminosity (which are measured). If the Kormendy relations for this sample are similar to that of normal elliptical galaxies, then these host galaxies are likely to be dynamically similar to normal galaxies.

Figure 2 shows the Kormendy relations for the host galaxies of the two subsamples (only 16 RLQs had published effective radii). Performing a two-dimensional K-S test (Fasano & Franceschini 1987), we find that these subsamples are consistent with having been drawn from the same parent distribution (40% probability). The best-fit linear relations are $\mu_e = (3.6 \pm 0.8)\ \log_{10}\ (r_e/\mathrm{kpc}) + (17.4 \pm 0.7)$ mag/arcsec^2. for the low-power subsample, and

$\mu_e = (2.75 \pm 1.2)\ \log_{10}\ (r_e/\mathrm{kpc}) + (18.6 \pm 1.0)$ mag/arcsec^2 for the high-power subsample. The quoted errors are the one-sigma confidence levels for the linear fit. No published errors were available for the high-power subsample, so a conservative 0.2 mag/arcsec^2 and 20% were used for μ_e and r_e respectively when calculating the linear fits. These two relations are consistent within error, and remain so even if we assume much smaller errors in μ_e and r_e for the high-power sample.

The R-band Kormendy relation for normal ellipticals in the local universe reported by Hamabe & Kormendy (1987) is $\mu_e = 2.94\ \log_{10}\ r_e + 18.4$, consistent within the errors with both the low- and high-power subsamples, especially if we take into account the evolution of the intercept with redshift (-0.3 to -0.4 mag/arcsec^2 at the median sample redshift of $z \sim 0.25$; Treu *et al.* 2001).

3.2. The Host Galaxy – Nucleus Link

Comparison of extended radio power between BL Lac objects and RLQs verifies their difference in intrinsic power. Extended radio power provides rough bolometer of time-integrated power of the nucleus, independent of relativistic beaming of the jet emission. The median extended radio power of the low-power sources is $\log_{10}\ P_{5GHz} = 24.3$ W Hz^{-1}, compared to $\log_{10}\ P_{5\mathrm{GHz}} = 26.7$ W Hz^{-1} for the high-power sources: a difference of 2.4 orders of magnitude. Over four orders of magnitude separate the least radio-powerful BL Lacs from the most radio-powerful RLQs. Yet host galaxy luminosities span less than one order of magnitude (~ 2 mag).

Extended radio power is partly dependent on the age of the source and on the properties of the host galaxy through which the radio-emitting jet must pass. A more direct measure of power of the nucleus is the total luminosity emitted by the nucleus, which can sometimes be estimated from its observed optical brightness. However, in BL Lac objects, strong relativistic beaming (which allowed us to select this matched redshift sample) enhances the perceived brightness by $\sim \delta^3$, where δ is the kinematic Doppler factor of the emitting jet plasma. To correct for beaming we use published estimates of Doppler factors from two blazar studies: Ghisellini *et al.* (1993), in which lower limits on the Doppler factor are calculated from measurements of bulk motion in the radio jet, and Dondi & Ghisellini (1995), in which lower limits to δ are calculated from measurements of the ratio of γ- to X-ray photons, assuming a synchrotron self-Compton model.

These two studies give lower limits of Doppler factors for eight of our 40 BL Lac objects. To estimate the nuclear brightnesses of the remaining sources we use the median value of

$\delta = 3.7$. This is both the median of the eight BL Lacs in this sample and also the median of the measured Doppler factors for the original HST-imaged sample of 110 BL Lacs, so is likely to be representative of the class. Although beaming may affect the luminosities of the RLQ sample to some degree, its effect will be small in comparison to the BL Lac objects given the dominance of the thermal emission associated with the accretion disk in RLQs.

Figure 3 shows absolute host galaxy magnitude versus absolute nuclear magnitude for the low- and high-power subsamples. The BL Lac nuclear magnitudes have been K corrected and corrected for beaming, with the lower limits in the Doppler factors translating to upper limits in nuclear luminosities. The median absolute nuclear magnitude for the 8 BL Lacs with measured Doppler factor limits is $M_R \gtrsim -19.23$ mag, while for the entire low-power subsample it is $M_R \gtrsim -17.59$ mag. For the high-power sources (K corrected only) the median absolute magnitude is -24.5 mag. At least four orders of magnitude separate the least powerful BL Lacs ($M_R \gtrsim -17$ mag) and the most luminous RLQs ($M_R \sim -27$ mag).

Although the host galaxies of the low-power sample span a similar range in magnitude to those of the high-power sample, they are on average slightly fainter. This leads to a shallow trend between the host galaxy and nuclear luminosities across the combined sample. We calculated the Kendall's τ correlation coefficient, censoring the upper limits in the beaming-corrected BL Lac nuclear luminosities (and for four of their host luminosities). The trend was significant for the case where we include the entire low-power subsample, beaming-corrected with the median Doppler factor (0.01% probability of no correlation; Kendall's (τ) for 62 points: 0.555), and for the case where we include only those of the low-power subsample with measured Doppler factor limits (0.5% probability of no correlation; Kendall (τ) for 30 points: 0.671).

Although this trend is statistically significant, it is also very shallow. Performing a linear fit with the high-power subsample combined with the non-beaming-corrected low-power subsample, we find that the host galaxy luminosity increases by only 1 mag for an increase of 7 mag in the luminosity of the nucleus. Any introduction of beaming correction decreases this gradient further. Applying the median Doppler factor corrections to the low-power subsample yields an increase in ~ 10 mag in the nuclear luminosity for each magnitude of host galaxy luminosity.

The shallowness of this trend, and the narrow range in luminosity exhibited by these host galaxies demonstrates that, for radio-loud AGN, the luminosity (and hence mass) of the host galaxy has little relation to the energy output of the nucleus. If the correlation between bulge luminosity and central black hole mass observed in nearby, non-active galaxies (Magorrian *et al.* 1998; van der Marel 1999a) also applies to these host galaxies, then this tight range of host luminosities implies a small range of (very high) black hole masses, and hence a very

large range of Eddington ratios. In the following sections we derive these Eddington ratios using two different methods for estimating the black hole masses.

3.3. Black Hole Masses and Eddington Ratios from Bulge Luminosity

Since the host galaxies of radio-loud AGN appear to be normal ellipticals in every respect measured (see Sect. 3.1), it is plausible that the AGN black hole mass and host galaxy luminosity are correlated, as observed in nearby, non-active galaxies (Magorrian *et al.* 1998; van der Marel 1999a). If so, radio-loud AGN are powered by very massive central black holes. We use the relation presented by Kormendy & Gebhardt (2001) to calculate these:

$$M_\bullet = 0.78 \times 10^8 M_\odot \frac{L_{B,bulge}}{10^{10} L_{B,\odot}} \ . \tag{1}$$

Assuming an early-type spectrum to derive $L_{B,bulge}$ from the R-band magnitudes (see Sect. 2.3), we find median black hole masses of $1.1 \times 10^9 M_\odot$ (mean: $1.2 \times 10^9 M_\odot$) for the low-power subsample, and $1.7 \times 10^9 M_\odot$ (mean: $2.0 \times 10^9 M_\odot$) for the high-power subsample, with standard deviations $6.8 \times 10^8 M_\odot$ and $1.0 \times 10^9 M_\odot$ respectively. The median for the entire sample is $M_\bullet = 1.2 \times 10^9 M_\odot$, with standard deviation $7.7 \times 10^8 M_\odot$ (mean: $1.2 \times 10^9 M_\odot$).

The upper part of Figure 4 shows the derived black hole masses versus (corrected) magnitude of the nucleus. The error in black hole mass is dominated by the scatter in the $M_\bullet$—L_{bulge} relation (the RMS dispersion is a factor of 2.8; Kormendy & Gebhardt 2001), but also affected by the uncertainty in the host galaxy magnitudes and in the spectral corrections (a factor of $\sim \pm 10\%$).

The shallow correlation noted between the luminosities of host galaxy and nucleus (Sect. 3.2) leads to a correlation between black hole mass and nuclear luminosity; however, when we include the error bars in the black hole masses, the correlation is not statistically significant.

Given AGN black hole masses estimated in this way, we can derive the Eddington luminosity:

$$L_{Edd} = \frac{4\pi G M_\bullet m_p c}{\sigma_T} \ , \tag{2}$$

where $M_\bullet$ is the black hole mass, m_p the mass of the proton, and σ_T the Thompson cross-

section. From this we calculate the Eddington ratio using the corrected nuclear magnitudes, assuming a spectral index of $\alpha = 1$ to estimate bolometric luminosity. The nuclear magnitudes of BL Lac objects are corrected for beaming using lower limits to the Doppler factors, meaning the calculated Eddington ratios are upper limits.

For the eight BL Lacs with measured Doppler factor limits, the median Eddington ratio limit is $\frac{L_{bol.}}{L_{Edd}} \lesssim 0.002$. For the entire low-power sample, corrected with the median Doppler factor, we obtain $\frac{L_{bol.}}{L_{Edd}} \lesssim 3 \times 10^{-4}$. The median Eddington ratio for the high-power sources is much higher, with $\frac{L_{bol.}}{L_{Edd}} = 0.1$. The upper part of Figure 5 shows the histogram of Eddington ratios (or Eddington ratio limits) for the reduced low-power sample and the high-power sample.

3.4. Black Hole Masses and Eddington Ratios from Velocity Dispersion Estimates

Black hole mass appears to be much more tightly correlated with velocity dispersion (σ_e) than with bulge luminosity (Gebhardt *et al.* 2000; Ferrarese & Merritt 2000; Kormendy & Gebhardt 2001). If we assume that our host galaxies lie on the Fundamental Plane for normal ellipticals, we can infer velocity dispersions using the measured values of r_e and $\langle I \rangle_e$ — the mean surface brightness within r_e. This assumption is reasonable, as we know that these host galaxies are indistinguishable from normal elliptical galaxies morphologically, and from § 3.1 we know that they are consistent dynamically, with their Kormendy relations matching.

We use the Fundamental Plane parameters measured by Jorgensen, Marijn & Kjaegaard (1995) from R-band photometry of a large sample of E and S0 galaxies across several clusters:

$$\log r_e = 1.24 \log \sigma_e - 0.82 \, \langle I \rangle_e + \gamma \ . \tag{3}$$

The evolution of the zero point, γ, with redshift is calculated using the measurements of Fundamental Plane parameters at different redshifts by Jorgensen *et al.* (1999), yielding $\gamma = 0.2132z - 1.31 \times 10^{-3}$.

The velocity dispersions derived were used to calculate black hole masses using the relation:

$$M_\bullet = 1.3 \times 10^8 M_\odot (\frac{\sigma_e}{200 \text{ km s}^{-1}})^{4.2} \ . \tag{4}$$

The value of the exponent is somewhat uncertain, with conflicting measurements in the literature. Kormendy & Gebhardt (2001) measure an $\alpha = 3.65$, while Merritt & Ferrarese (2001) measure $\alpha = 4.72$. To reflect this uncertainty, we adopt a mean value of $\alpha = 4.2$ with an uncertainty equal to the standard deviation of the two values: ± 0.75.

The median black hole masses derived using this method are, for the low-power sample: $M_\bullet = 1.1 \times 10^9 M_\odot$ (mean: $1.8 \times 10^9 M_\odot$); and for the high-power sample: $M_\bullet = 4.6 \times 10^8 M_\odot$ (mean: $2.0 \times 10^9 M_\odot$). Black hole masses derived with this method show a greater spread than those derived using the $M_\bullet$—L_{bulge} relation, with standard deviations $2.3 \times 10^9 M_\odot$ and $3.0 \times 10^9 M_\odot$ respectively. The median for the entire sample is $M_\bullet = 1.0 \times 10^9 M_\odot$(mean: $8.9 \times 10^8 M_\odot$), with standard deviation $2.5 \times 10^9 M_\odot$.

The lower part of Figure 4 shows black hole mass versus the magnitude of the nucleus for the masses derived in this section. The errors in the black hole masses are dominated by the scatter in the Fundamental Plane relation, which is around 25% in σ_e for a given μ_e and r_e. The uncertainty in μ_e and r_e affect the errors to a lesser extent, and the errors in the actual Fundamental Plane fit parameters are small in comparison. The assumed error in α, although leading to differences of only $\sim \pm 15\%$ in black hole mass, compounds with the error in σ_e. As a result, although the scatter in the $M_\bullet$—σ_e relation is small, the final errors in the black hole masses calculated by this method are of similar order to those calculated from the $M_\bullet$—L_{bulge} relation. Again, taking these errors into account, there is no statistically significant trend between black hole masses derived in this section and nuclear luminosity, beaming corrected or otherwise.

The median Eddington ratio limit for the eight BL Lacs with measured Doppler factor limits is $\frac{L_{bol.}}{L_{Edd}} \lesssim 0.01$, while the median for the entire low-power subsample is $\frac{L_{bol.}}{L_{Edd}} \lesssim 3 \times 10^{-4}$. Again, these Eddington ratios are a great deal smaller than the median for the high-power sample calculated by this method: $\frac{L_{bol.}}{L_{Edd}} \lesssim 0.4$. The lower part of figure 5 shows the histogram of the Eddington ratios calculated in this section.

4. Discussion

The results from the two methods of black hole mass calculation agree: radio-loud AGN are powered by very massive central black holes, typically with $M_\bullet > 10^8 M_\odot$, and more often with $M_\bullet \sim 10^9 M_\odot$.

These results are generally consistent with the black hole masses derived for luminous radio-loud AGN in other studies. Falomo, Kotilainen & Treves (2002) find masses in the range $5 \times 10^7 M_\odot$ to $9 \times 10^8 M_\odot$ for their sample of 7 low-redshift ($z < 0.055$) BL Lacs,

calculated from spectroscopic measurements of stellar velocity dispersion. These fall within the range of masses found for our sample of BL Lacs via the velocity dispersion relation, although they tend toward the low-mass end of that range. This may indicate an evolutionary or selection effect between the two epochs studied. McLure & Dunlop (2001) find black hole masses in the range $2\times10^8 M_\odot$ to $2\times10^9 M_\odot$ for a sample of 22 radio-loud quasars, determined through reverberation mapping. These are consistent with the masses found for our high-power sample.

Our results support the idea that, although some radio-quiet objects may host very massive central black holes (Dunlop et al. 2002), luminous radio sources may require them. Dunlop et al. suggest a black hole mass threshold for radio-loud AGN of $5 \times 10^8 M_\odot$, which is supported by the black hole masses derived from bulge luminosity in this study. Masses derived in this study via the $M_\bullet$—σ_e relation suggest a threshold of $\sim 1\times10^8 M_\odot$. Whatever its value, we find that neither the threshold nor the distribution of black hole masses in radio-loud AGN depends on the actual level of radio emission, within the range represented by these radio sources, or on the overall energy output of the nucleus.

As a consequence, radio-loud AGN exhibit an extremely broad range of accretion rates; from $\frac{L_{bol.}}{L_{Edd}} \lesssim 2 \times 10^{-4}$ to $\frac{L_{bol.}}{L_{Edd}} \sim 1.0$. Across this range the host galaxies span a remarkably tight range of high stellar luminosities — all within one magnitude of brightest cluster galaxies — suggesting that, at least for radio-loud AGN, there is at most a very weak relation between the properties of the host galaxy and both the overall rate and the efficiency of fuelling of the black hole.

5. Conclusions

We find that the host galaxies of radio-loud AGN are luminous ellipticals, occupying the low surface-brightness tail of the Kormendy relation for normal elliptical galaxies, and are statistically consistent with this relation. Comparing the host galaxies of low-power and high-power radio-loud AGN, we find general overlap, with a slight difference in median absolute Cousins R magnitudes, -23.75 mag and -24.2 mag, respectively. After correcting the (highly beamed) low-power AGN for Doppler beaming, we find a significant positive trend between nuclear and host galaxy luminosity, but with a very shallow slope — a factor of 1.3 in host galaxy brightness over at least four orders of magnitude in nuclear luminosity — ruling out a close relation between host galaxy and nuclear luminosity in radio-loud AGN.

We find that the central black holes of luminous radio-loud AGN are universally large, with median black hole mass $\sim 10^9 M_\odot$ for this sample. This is found to be the case using

either the $M_\bullet$—L_{bulge} relation and the $M_\bullet$—σ_e relations to derive black hole masses. This supports the view that a high central black hole mass is an important factor in generating a powerful radio source.

No correlation is found between black hole mass and energy output from the nucleus. Rather, the black hole masses derived span a surprisingly small range compared to the range in intrinsic power of this sample. Eddington ratios for radio-loud AGN span more than four orders of magnitude, with $\frac{L_{bol.}}{L_{Edd}} \lesssim 2 \times 10^{-4}$ in the lowest-power sources to $\frac{L_{bol.}}{L_{Edd}} \sim 1$ in the highest. Across this range, the host galaxies luminosities are tightly constrained, all within one magnitude of brightest cluster galaxies. Thus, although the properties of the host galaxy may have a strong influence the mass of its central black hole, they have at most a very weak influence on the mass accretion rate in radio-loud AGN.

We thank Aldo Treves and Laura Maraschi for very helpful discussions. Support for this work was provided by NASA through grant numbers GO-05938.01-94A, GO-05939.01-94A, GO-06363.01-95A and GO-07893.01-96A from the Space Telescope Science Institute, which is operated by AURA, Inc., under NASA contract NAS5-26555.

REFERENCES

Bahcall, J. N., Kirhakos, S., Saxe, D. H. & Schneider. D. P. 1997 ApJ 479, 642

Barthel, P. 1989 SciAm 260, 20

Boyce, P. J., Disney, M. J., Blades, J. C., *et al.* 1998 MNRAS 298, 121

Bressan, A., Chiosi, C. & Fagotto, F. 1994 ApJs 94, 63

Bruzual & Charlot 1993 ApJ 405, 538

Dondi, L. & Ghisellini, G. 1995 MNRAS 273, 583

Dunlop, J. S., McLure, R. J., Kukula, M. J., et al. 2002 MNRAS, in press

Efstathiou, G., Ellis, R. S. & Peterson, B. A. 1988 MNRAS 232, 431

Fasano, G.& Franceschini, A. 1987 MNRAS 225, 155

Falomo, R., Kotilainen, J. K. & Treves, A. 2002 ApJ Letters, in press

Ferrarese, L. & Merritt, D. 2000 ApJ 539, L9

Gebhardt, K., Bender, R., Bower, G., *et al.* 2000 ApJ 539, L13

Ghisellini, G., Padovani, P., Celotti, A. & Maraschi, L. 1993 ApJ 407, 65

Haehnelt, M. G. & Rees, M. J. 1993 MNRAS 263, 168

Hamabe, M. & Kormendy, J. 1987 in IAU Symp. 127, Structure and Dynamics of Elliptical Galaxies, ed. P. T. de Zeeuw (Dordrecht: Kluwer), 379

Ho, L. 1999 in Observational Evidence for Black Holes in the Universe, ed. S. K. Chakrabarti (Dordrecht: Kluwer), 157

Hooper, E. J., Impey, C. D. & Foltz, C. B. 1997 ApJ 480, L98

Jorgensen, I., Marijn, F. & Kjaegaard, P. 1995 MNRAS 276, 1341

Jorgensen, I., Marijn, F., Jens, H. & van Dokkum, P. G., 1999 MNRAS 308, 833

Kauffmann, G. & Haehnelt, M. G. 2000 MNRAS 311, 576

Kellerman, K. I., Sramek, R., Schmidt, *et al.* 1989 AJ 98, 1195

Kormendy, J. 1977 ApJ 218, 333

Kormendy, J. & Gebhardt, K. 2001 in The 20th Texas Symposium on Relativistic Astrophysics, ed H. Martel & J. C. Wheeler (AIP)

Magorrian, J., Tremaine, S., Richstone, D. *et al.* 1998 AJ 115, 228

McLeod, K. K., Rieke, G. H. & Storrie-Lombardi, L. J. 1999 ApJ 511, L67

McLure, R. J., Kukula, M. J. & Dunlop, J. S. 1999 MNRAS 308, 377

McLure, R. J., Dunlop, J. S. & Kukula, M. J. 2000 MNRAS 318, 693

McLure, R. J. & Dunlop, J. S. 2002 MNRAS, in press

Merritt, D. & Ferrarese, L. 2001 MNRAS.320, L30

Padovani, P. & Giommi, P. 1995 ApJ 444, 567

Pentericci, L., McCarthy, P. J., Röttgering, H. J. A., Miley, G. K., van Breugel, W. J. M. & Fosbury, R. 2001 ApJS 135, 63

Ridgway, S. E., Stockton, A. 1997 AJ 114, 511

Scarpa, R., Urry, C. M., Falomo, R., Pesce, J. & Treves, A. 2000 ApJ 532, 740

Scarpa, R., Urry, C. M., Padovani, P., Calzetti, D., O'Dowd, M. 2000 ApJ 544, 258

Schade, D. J., Boyle, B. J. & Letawsky, M. 2000 MNRAS, 315 & 498

Small & Blandford 1992 MNRAS 259, 725

Smith, E. P. & Heckman T. M. 1990 ApJS 69, 365

Smith, E. P., Heckman, T. M., Bothun, G. D., Romanishin, W. & Balick, B. 1986 ApJ 306, 64

Thuan, T. X. & Puschell, J. J. 1989 ApJ 346, 34

Treu, T., Stiavelli, M., Bertin, G., *et. al* 2001 MNRAS 326, 237

Urry, C. M. & Padovani, P. 1995, PASP 107, 803

Urry, C. M., Scarpa, R., O'Dowd, M., *et al.* 2000, ApJ 532, 816

van der Marel, R. P. 1999, AJ 117, 744

van der Marel, R. P. 1999 in ASP Conference Series 182, Galactic Dynamics, ed. D. R. Merritt, M. Valluri, and J. A. Sellwood, (San Francisco: ASP)

AAS LaTeX macros v5.0.

Table 1. The High-Power Sample*

Name	z	M_R(host)	M_R(nucl.)	R_e(kpc)	P_{5GHz}(log W Hz^{-1})
Dunlop et al. (2002)					
0137+012	0.258	-24.47	-23.50	15.16	26.78
0736+017	0.191	-23.95	-24.05	13.96	26.81
1004+130	0.240	-24.58	-25.75	8.71	26.40
2141+175	0.213	-23.91	-24.49	8.65	26.33
2247+140	0.237	-24.22	-23.82	14.34	26.77
2349-014	0.173	-24.66	-24.04	20.06	26.24
1020-103	0.197	-23.77	-23.37	7.46	26.13
1217+023	0.240	-24.74	-23.74	11.80	26.45
2135-147	0.200	-24.40	-23.40	12.20	26.67
2355-082	0.210	-23.23	-23.62	10.97	25.96
Boyce et al. (1998)					
0202-760	0.389	-22.93	-23.95	3.85	27.30
3C351	0.371	-24.28	-25.15	6.26	26.90
0312-770	0.223	-23.56	-22.76	18.61	26.43
Hooper, Impey & Foltz (1997)					
1138+0003	0.500	-24.57	-24.38	—	25.48
1218+1734	0.445	-23.84	-23.72	—	25.20
1222+1235	0.412	-24.34	-24.05	—	25.06
1230-0015	0.470	-24.71	-24.68	—	25.65
2348+0210	0.504	-24.36	-25.16	—	25.45
2351-0036	0.460	-23.52	-24.22	—	26.27
Bahcall et al. (1997)					
1004+130	0.240	-24.37	-25.84	9.37	27.26
3C273	0.158	-24.43	-27.20	18.33	28.41
1302-102	0.286	-23.50	-26.27	10.45	26.40
3C323.1	0.266	-23.39	-24.56	14.01	26.95
2135-147	0.200	-23.45	-25.12	16.63	27.02
2349-014	0.173	-24.44	-25.01	26.23	26.40

*These values have been converted from the published values to our adopted cosmology, $H_0 = 50$ km/s/Mpc and $q_0 = 0$, and in the case of magnitudes, to Cousin's R band.

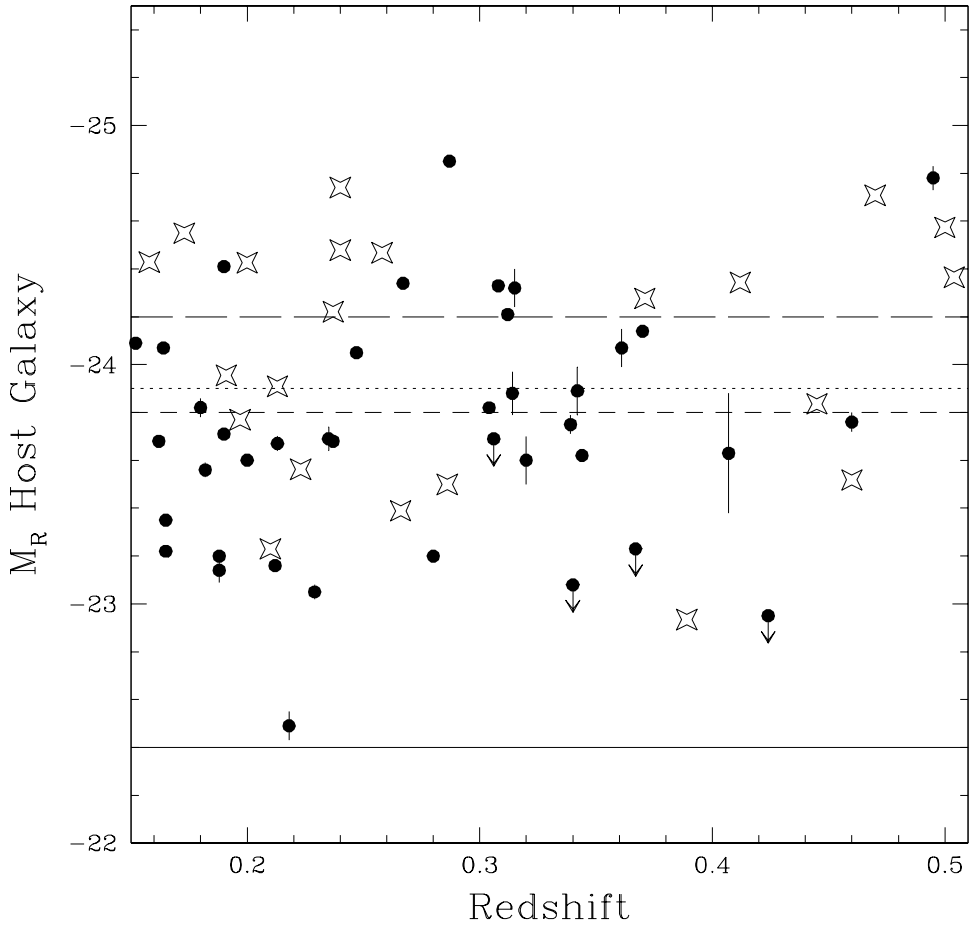

Fig. 1.— The K-corrected absolute R-band magnitudes of the host galaxies of low-power radio-loud AGN (*circles*) and high-power radio-loud AGN (*stars*) largely overlap over the redshift range studied – $0.15 \leq z \leq 0.5$. Overall, the host galaxies of high-power AGN are slightly brighter, with median brightness $M_R = -24.2 \pm 0.5$ mag (*long-dashed line*) compared to $M_R = -23.75 \pm 0.5$ mag for the low-power AGN (*short-dashed line*). A K–S test indicates a marginal difference between the host galaxy magnitudes (4% probability of being drawn from the same distribution). The *solid line* shows the characteristic value for normal ellipticals ($L^* = -22.4$ mag; Efstathiou, Ellis & Peterson 1988), while the *dotted line* shows the average magnitude of brightest cluster galaxies (−23.9 mag; Thuan & Puschell 1989).

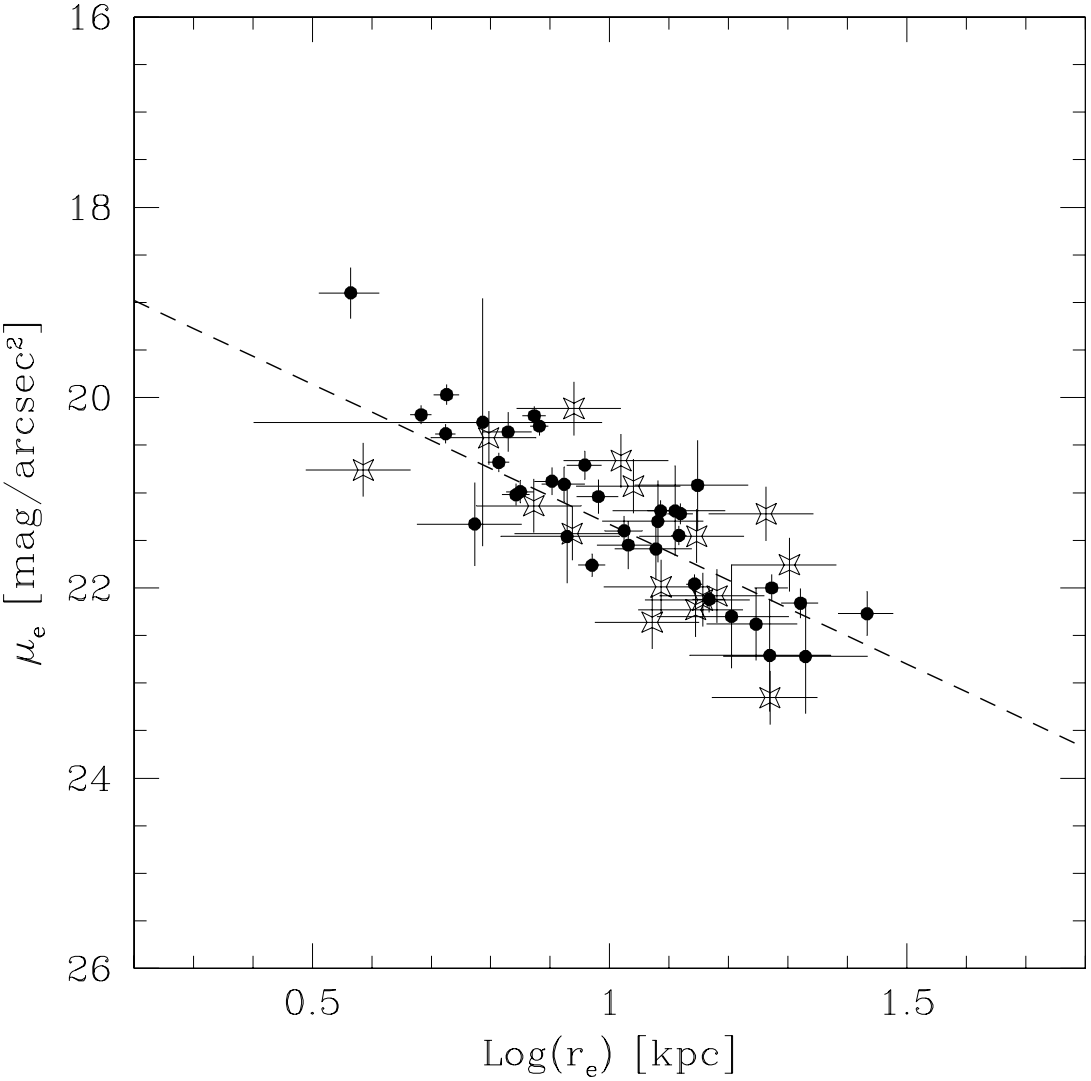

Fig. 2.— Surface brightness versus effective radius for the host galaxies of low-power radio-loud AGN (*circles*) and high-power radio-loud AGN (*stars*). The best-fit Kormendy relations for the two samples are consistent with each other, and both are consistent with the Kormendy relation derived by Hamabe & Kormendy (1987) for normal elliptical galaxies (*dashed line*). This suggests that the radio-loud AGN host galaxies in this sample are dynamically similar to normal elliptical galaxies.

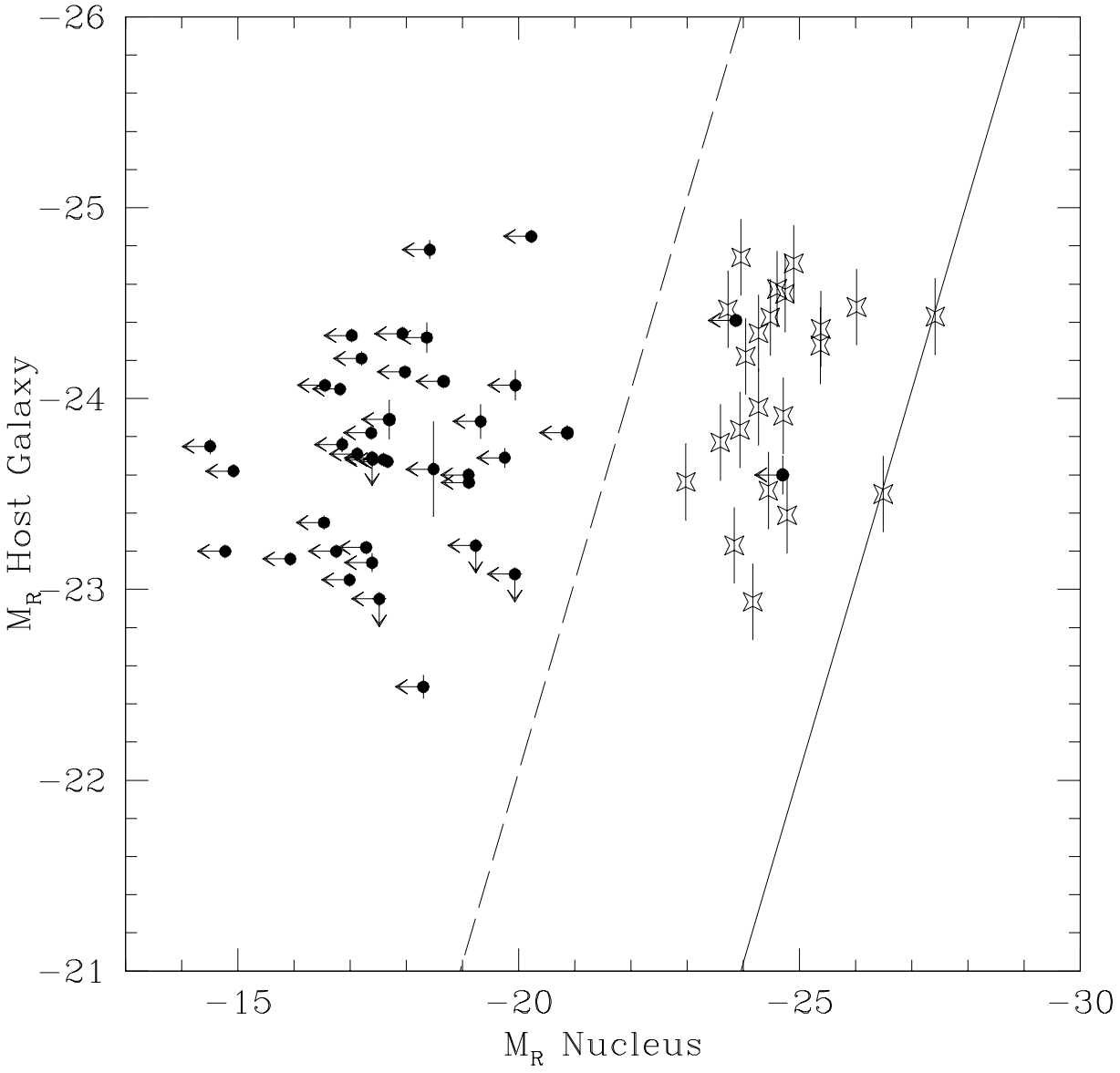

Fig. 3.— Absolute R-band host galaxy versus nuclear magnitude (K-corrected and, for BL Lac nuclei, also corrected for beaming) for low-power radio-loud AGN (*circles*) and high-power radio-loud AGN (*stars*). The scatter in the host galaxy magnitudes is small (RMS is 0.6 mag), compared to more than 4 orders of magnitude in nuclear luminosity between the least luminous BL Lac nuclei and the most luminous RLQs. There is a statistically significant trend between host galaxy and nuclear magnitude, but it is considerably shallower than the line of constant Eddington ratio (*solid line* is $L/L_{Edd} = 1$, *dashed line* is $L/L_{Edd} = 0.01$) obtained by assuming the host galaxy luminosity–black hole mass relation reported by Kormendy & Gebhardt (2001).

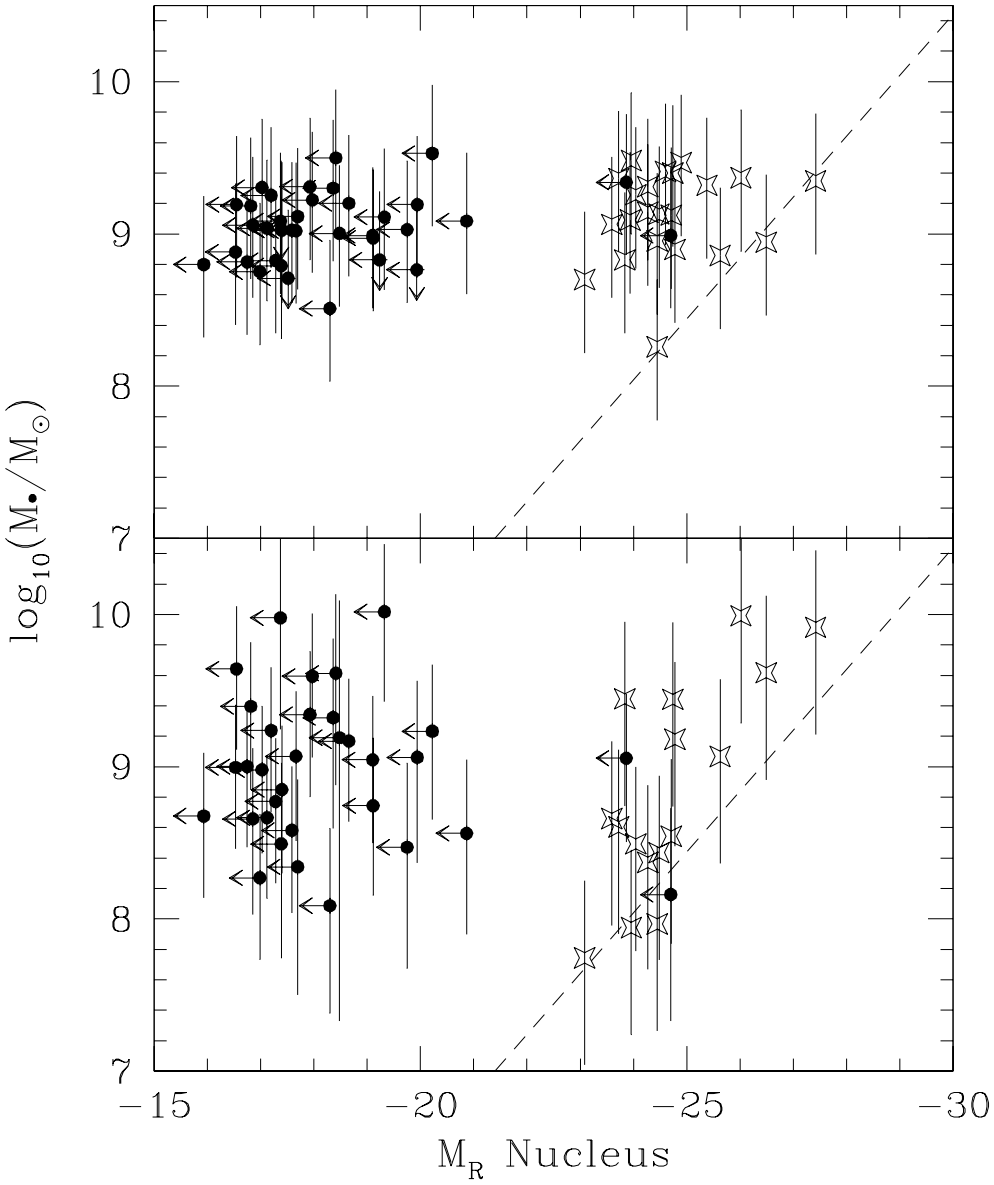

Fig. 4.— Derived black hole masses versus nuclear magnitude (again, K-corrected and, for BL Lac nuclei, corrected for beaming) for low-power radio-loud AGN (*circles*) and high-power radio-loud AGN (*stars*). *Upper plot:* using the bulge luminosity correlation (Magorrian *et al.* 1998; Kormendy & Gebhardt 2001). *Lower plot:* using the stellar velocity dispersion correlation (Gebhardt *et al.* 2000; Ferrarese & Merritt 2000; Kormendy & Gebhardt 2001) combined with the Fundamental Plane relation (Jorgensen, Marijn & Kjaegaard 1995). Both plots suggest that these radio-loud AGN exhibit a relatively small range of high black hole masses for a very large range (> 4 orders of magnitude) in energy output from the nucleus. Although radio-loud AGN can extend to very faint nuclear magnitudes, they appear to be cut off at the bright end by an envelope consistent with the Eddington luminosity (*dashed line*).

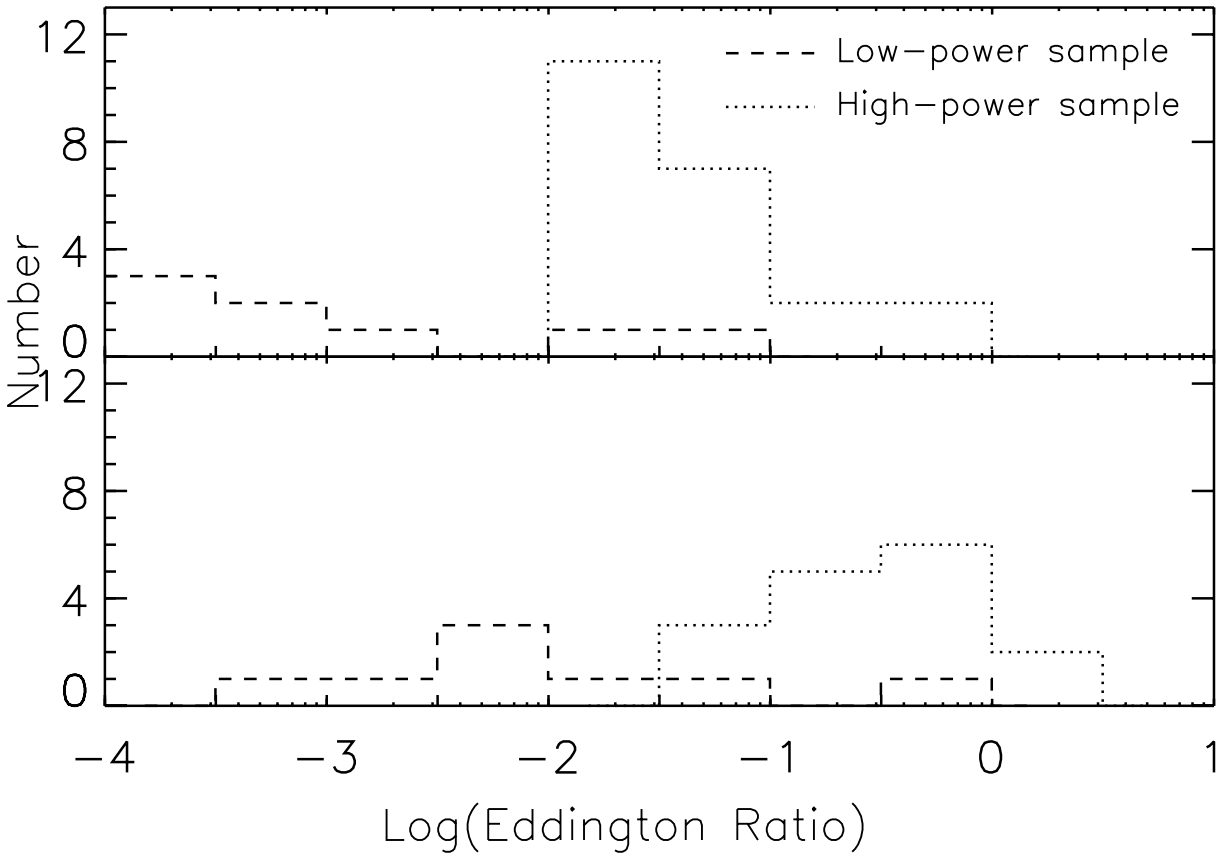

Fig. 5.— Histogram of Eddington ratios for low- and high-power radio-loud AGN (including only the eight low-power sources with measured Doppler factors). Black hole masses are calculated from the bulge luminosity relation (*upper histogram*) and from the velocity dispersion relation (*lower histogram*).